

Cosmic Growth and Expansion Conjoined

Eric V. Linder^{1,2}

¹*Berkeley Center for Cosmological Physics & Berkeley Lab,
University of California, Berkeley, CA 94720, USA*

²*Energetic Cosmos Laboratory, Nazarbayev University, Astana, Kazakhstan 010000*

(Dated: September 10, 2018)

Cosmological measurements of both the expansion history and growth history have matured, and the two together provide an important test of general relativity. We consider their joint evolutionary track, showing that this has advantages in distinguishing cosmologies relative to considering them individually or at isolated redshifts. In particular, the joint comparison relaxes the shape degeneracy that makes $f\sigma_8(z)$ curves difficult to separate from the overall growth amplitude. The conjoined method further helps visualization of which combinations of redshift ranges provide the clearest discrimination. We examine standard dark energy cosmologies, modified gravity, and “stuttering” growth, each showing distinct signatures.

I. INTRODUCTION

The histories of the expansion of the universe and the growth of large scale structures within it are key observables that provide insights into the cosmological model. In particular, within general relativity the two are tightly tied together, even more so within models close to the concordance cosmological constant plus cold dark matter, Λ CDM. In standard models, these histories are quite smooth and gently varying, generally on a Hubble expansion timescale, and thus discriminating between cosmologies is not easy, even with reasonably precise measurements. That is, one does not have sharp or oscillating features the way one does when analyzing, for example, cosmic microwave background (CMB) power spectra.

Although the amplitudes of the growth or growth rate history, for example, may differ between cosmologies, this is often nearly degenerate with the initial conditions of the mass fluctuations, or the present mass fluctuation amplitude σ_8 . Without a clear distinction in the shape of the history curve over the epochs where precise data exists, this makes cosmological characterization problematic.

We therefore seek a way to interpret the data such that the difference in the shapes of the evolutionary tracks becomes more pronounced. The simple solution we find is to contrast the expansion history in terms of the Hubble expansion rate $H(z)$ directly with the growth history in terms of the growth rate $f\sigma_8(z)$, rather than each as a function of redshift. Just as the tracks in a Hertzsprung-Russell (HR) diagram of luminosity vs temperature, or a supernova plot of magnitude vs color, can illuminate the physics more clearly than plotting either vs its dependent variable (age or time), so too do the cosmic histories when plotted against each other rather than as a function of time or redshift. Of course no extra physics is added by this change in visualization, just readier recognition, identification, and interpretation of the existing physics, i.e. deviations from general relativity or standard cosmology and particular redshift ranges of interest.

In Sec. II we exhibit the difficulties in distinguishing cosmologies in the standard approach of the evolution-

ary tracks vs time, as well as a new combination of both histories. We introduce the HR-type approach of considering histories conjointly in Sec. III and investigate it for several types of cosmologies, including quintessence, modified gravity, and stuttering growth. Section IV discusses the impact of future measurements on exploring the cosmic expansion and growth histories, and we conclude in Sec. V.

II. HISTORIES VS TIME

The expansion history can be most directly considered in terms of the Hubble expansion rate $H(z) = \dot{a}/a$, where $a = 1/(1+z)$ is the cosmic scale factor and z is the redshift. The Hubble parameter sets the scale for cosmic distances and age. Distances are integrals over the expansion history so $H(z)$ is more incisive concerning the conditions at a given redshift. The growth history similarly is best examined by means of an instantaneous quantity, the growth rate $f = d \ln D / d \ln a$, where $D(z)$ is the overall growth factor from some initial condition to a redshift z .

In fact, observations are sensitive to a product $f\sigma_8 \propto fD$, where $\sigma_8(z)$ measures the rms mass fluctuation amplitude at redshift z . Remarkably, measurements of the clustering of large scale structure provide both H and $f\sigma_8$, so a cosmic redshift survey delivers both the expansion history and growth history. The expansion rate comes from using the baryon acoustic oscillations in the clustering pattern as a standard ruler, and in particular the radial distances measure $H(z)r_d$, where r_d is the sound horizon at the baryon drag epoch in the early universe. The growth rate comes from redshift space distortions of the clustering pattern, caused by the (gravitationally induced) velocities of the galaxies or other tracers.

Both $H(z)$ and $f\sigma_8(z)$ tend to be smooth, slowly varying functions. In particular, $H(z)$ is generally monotonic and changes on a Hubble, or e-folding, time scale, while $f\sigma_8(z)$ has a broad peak which means that its value changes little during recent cosmic history where the data

is best measured. Figure 1 shows $H(z)$ for several models while Fig. 2 illustrates the properties of $f\sigma_8(z)$ for the same models.

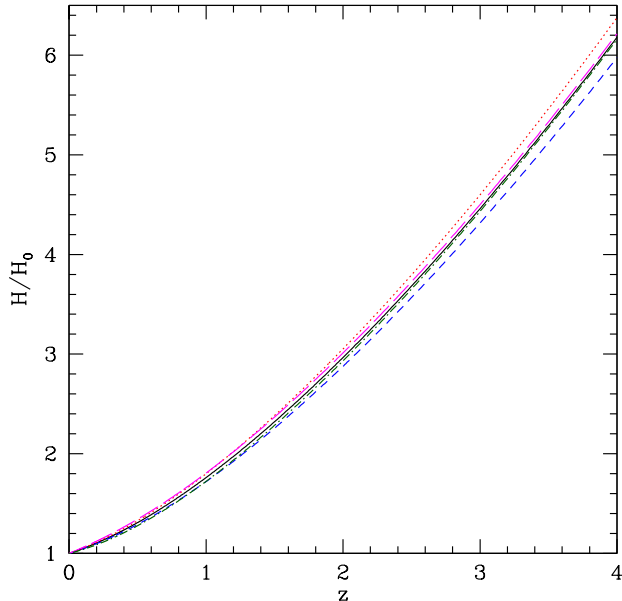


FIG. 1. The Hubble expansion parameter $H(z)/H_0$ is plotted as a function of redshift for cosmological models with matter density $\Omega_m = 0.28, 0.3, 0.32$ (blue dashed, black solid, red dotted curves respectively) for LCDM ($w = -1$), plus $w = -0.9, -1.1$ (magenta long dashed and green dot-dashed curves respectively) for $\Omega_m = 0.3$. The curves are smooth without localized features and degeneracies are apparent.

Note that not only is $f\sigma_8(z)$ reasonably constant, but the shapes of the curves for different cosmologies are fairly similar, mostly being simply offsets in amplitude. That is, they have different rms mass fluctuation amplitudes at present, σ_8 , but otherwise look similar for different cosmological physics. Standard models will have this broad peak due to simple physical constraints: at high redshift, in the matter dominated era, $f \rightarrow 1$ and $D \rightarrow a$ so $f\sigma_8 \propto a$ independent of model specifics. The linear increase with a in $f\sigma_8$ is counteracted at recent times by the suppression of growth caused by accelerating expansion – this reduces f below 1 and causes D to grow more slowly so the net effect is a gradual turnover during the accelerating epoch.

This lack of strong, cosmology dependent features in H and $f\sigma_8$ is disappointing since recent redshift surveys such as BOSS [1–11] and WiggleZ [12–14] have demonstrated precision measurements of these quantities and next generation spectroscopic surveys such as PFS, DESI, Euclid, and WFIRST will greatly improve on this. While a full statistical analysis will constrain the cosmological parameters, the visual “smoking gun” of a deviation from the standard model may not be apparent, and the results may depend more on the parametrization and

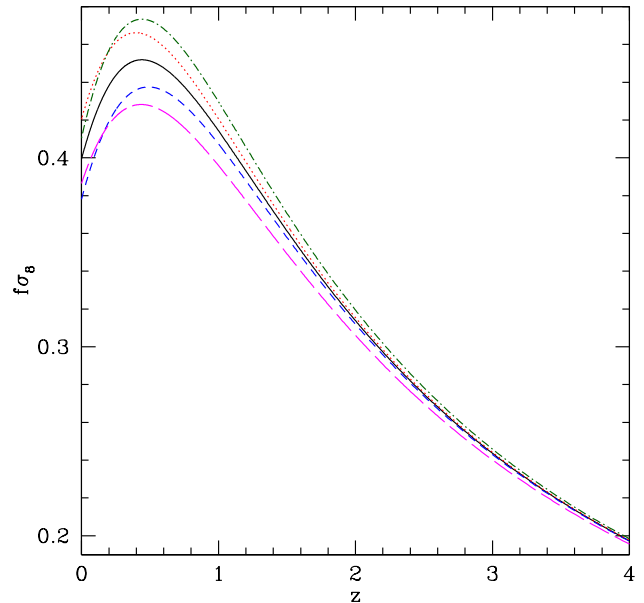


FIG. 2. As Fig. 1 but plotting the growth rate $f\sigma_8$ as a function of redshift. The models show more discrimination but at $z \approx 0.5-1.5$ are mostly similar shapes with scaled amplitudes.

the build up of signal to noise over redshift range. Thus, the motivation exists to find a more incisive, ideally visually clear method of using this expansion and growth data to discriminate between cosmologies.

In general relativity, expansion and growth are tied together, with expansion (and any microphysics such as sound speed) determining growth. That is, the linear growth equation depends solely on $H(z)$ and the present matter density. However, cosmologies where accelerated expansion is caused by extensions to Einstein gravity generally break this close relation, allowing for greater changes to the H and $f\sigma_8$ histories. This suggests that simultaneous consideration of these two functions may give greater insight. This has been explored, with some interesting results, at individual redshifts, i.e. the expansion at redshift z_1 vs the growth at redshift z_1 [1, 15–19].

Here we extend this to conjoint investigation of expansion and growth as full functions, i.e. their histories or evolutionary tracks. The first thing one might try, motivated by the above discussion about the generic behavior of $f\sigma_8$ (and H) in the matter dominated era, is to combine the functions together. We have good reasons to believe that a matter dominated era must exist, whatever the late time cosmology: breaking matter domination would give a huge Sachs-Wolfe effect on the CMB in contradiction to observations, plus severely impact the formation of large scale structure. Figure 1 of [20] shows the dramatic effect of even 0.1 e-fold of early acceleration on the CMB.

Given early matter domination, recall that $f\sigma_8 \propto a$ and $H^2 \propto a^{-3}$. This suggests that all reasonable cos-

mologies should go to $f\sigma_8 H^{2/3} = \text{constant}$ during that epoch. To investigate whether convolving the expansion and growth histories in such a way improves distinction between models, we plot this combination vs redshift in Fig. 3.

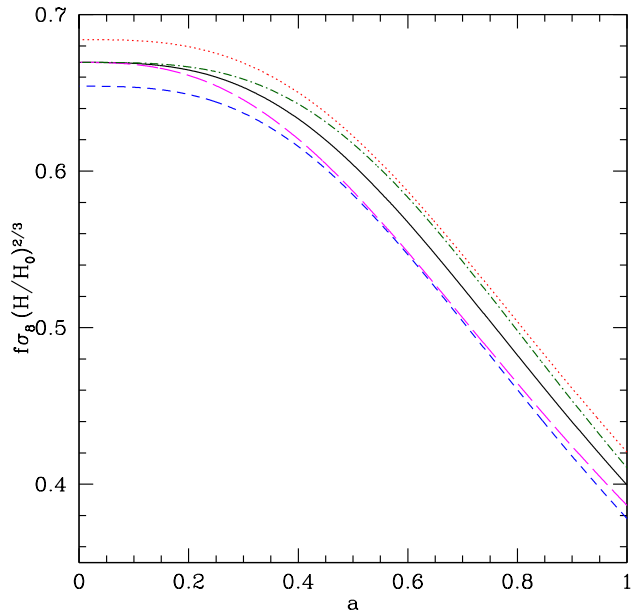


FIG. 3. The combination $f\sigma_8(H/H_0)^{2/3}$ is plotted vs scale factor for the models in Fig. 1. This combination goes to a constant at high redshift (small a). This constancy provides an important test of early matter domination and general relativity, but is at redshifts $z \gtrsim 4$ where observations are difficult. At redshifts $z \lesssim 1.5$, the degeneracy between Ω_m and w is apparent, so measurements out to $z \approx 3$ are important.

The evolutionary tracks are quite similar, lying in a fairly narrow band. In particular, the curve shapes do not have any distinguishing features. The amplitudes go to a constant involving $(\Omega_m h^2)^{2/3} A_s^{1/2}$ at high redshift, where A_s is the scalar perturbation power amplitude of the CMB. Since the CMB similarly tightly constrains the combination $\Omega_m h^2$, models start out at small a close together and are mostly affected by more recent growth effects such as suppression from cosmic acceleration. Because of the lack of shape features, the $f\sigma_8 H^{2/3}$ test seems better suited as a consistency test, though precision data during the high redshift ($z \gtrsim 3$) constant regime is difficult to obtain.

The approach in the next section appears much more promising to discriminate visually between cosmologies.

III. HISTORY VS HISTORY

Another approach to conjoint analysis of the expansion and growth histories is, rather than combining the functions, to contrast them. That is, consider the histories as

a function of each other, rather than of time for either the individual or convolved histories. The time dependence will run along the curves in the two dimensional space of expansion vs growth, or more specifically H vs $f\sigma_8$.

Figure 4 shows that this has useful characteristics, including a fairly well defined bump or wiggle that could clarify visually distinctions between cosmological models. Moreover, the interpretation in terms of physics remains in the forefront: e.g. for a given expansion rate (horizontal cut), the growth rate is seen to be enhanced or suppressed relative to a fiducial model. Because the axes involve rates, this gives a focused view rather than being complicated by inertia from earlier or later conditions, as the overall growth factor or distances would be.

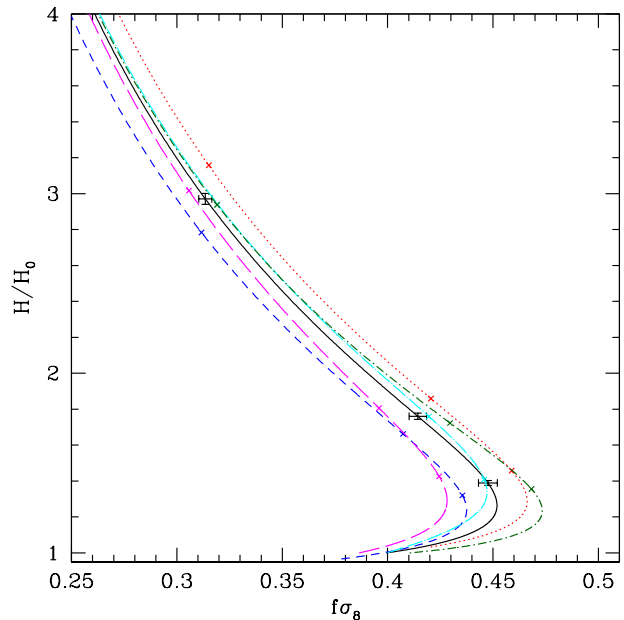


FIG. 4. The expansion rate $H(z)/H_0$ and growth rate $f\sigma_8$ are plotted against each other for the cosmological models in Fig. 1. Redshift, or scale factor, runs along the curves; small x's indicate $z = 0.6, 1, 2$ along the individual curves (from bottom to top). The cyan, dot-long dash curve is a mirage dark energy model. Plotted jointly, the expansion history and growth history exhibit more definite curvature, and discrimination beyond $z \gtrsim 1.5$. Error bars along the $\Omega_m = 0.3$ LCDM (solid black) curve indicate 1% uncertainties in measurements of expansion and of growth at $z = 0.6, 1, 2$.

The models have been normalized to all have the same $\Omega_m h^2$, which is well measured by the CMB. Thus at high redshift the tracks are all parallel to each other. While the y-axis is labeled as H/H_0 , this is actually the H_0 of the $\Omega_m = 0.3$ model, so models with different Ω_m have $H(z=0)/H_0 = (0.3/\Omega_m)^{1/2}$ rather than unity. At intermediate redshifts, the history vs history tracks show a prominent wiggle in the range $z \approx 0.4 - 1$. Since such a feature aids distinction between models, this approach is particularly useful since this region has the most accurate measurements with current, and much future, data.

Shifts in the dark energy equation of state do not behave substantially differently from shifts in the matter density. This holds as well for a time evolving equation of state; the mirage dark energy model with strong evolution $(w_0, w_a) = (-0.8, -0.732)$ that nevertheless matches the CMB distance to last scattering of the Λ CDM model [21] lies within the envelope defined by the $w = -0.9$ and $w = -1.1$ curves over the redshift range plotted. This means that most viable standard models, i.e. within general relativity and not too far from Λ CDM, have roughly the same shape and lie within a band around the fiducial model. They mostly differ in the exact degree and location of the wiggle.

Next we consider models that enhance or suppress growth relative to standard models within general relativity. First we examine a modified gravity model, the exponential $f(R)$ gravity of [22] with $c = 3$. This has an expansion history extremely close to that of Λ CDM but has the generically enhanced growth of scalar-tensor gravity. Figure 5 illustrates a strong effect on the wiggle feature, with an enhanced growth rate at constant expansion rate (note the x's of the modified gravity model are horizontally aligned with the Λ CDM model with the same matter density). Note that the wiggle would veer even further to the right if we showed this model with the fiducial $\Omega_m = 0.3$ rather than $\Omega_m = 0.28$ as used. That is, already with $\Omega_m = 0.28$ the $f(R)$ track and its wiggle sweep all the way from the leftmost standard curve past the rightmost one. Thus, such a modified gravity model should be clearly distinguishable – especially with low redshift measurements.

Modified gravity models in general have scale dependent growth as well. Figure 5 illustrates this by showing the history vs history tracks for two different values of the density perturbation wave number, $k = 0.02$ and $0.1 h/\text{Mpc}$. At high redshift, the modified gravity theory acts like general relativity but deviates more recently in the low Ricci scalar curvature regime. On larger scales (smaller k) the deviation in growth at low redshift is more mild as scalar-tensor theories generally involve k^2 corrections to Einstein gravity. This gives the characteristic enhanced, late, scale dependent wiggle seen in Fig. 5. Note that the expansion histories remain identical, to each other and to $\Omega_m = 0.28$ Λ CDM, as shown by the x's lined up horizontally at the same values of $H(z)/H_0$. Thus, signatures of modified gravity are particularly visible in this expansion history vs growth history plane.

The opposite case of suppressed growth is more difficult to achieve within modified gravity for the standard expansion history (since scalar-tensor theories generate additional attractive forces that enhance growth). Instead, we use the superdecelerating dark energy model of [20, 23]. This is purely phenomenological and involves a period of enhanced dark energy density with $w = -1$ at early times (though still too little to affect significantly the CMB or cause an epoch of early acceleration) then a step up to the maximal equation of state $w = +1$ for a standard scalar field, in order to dilute

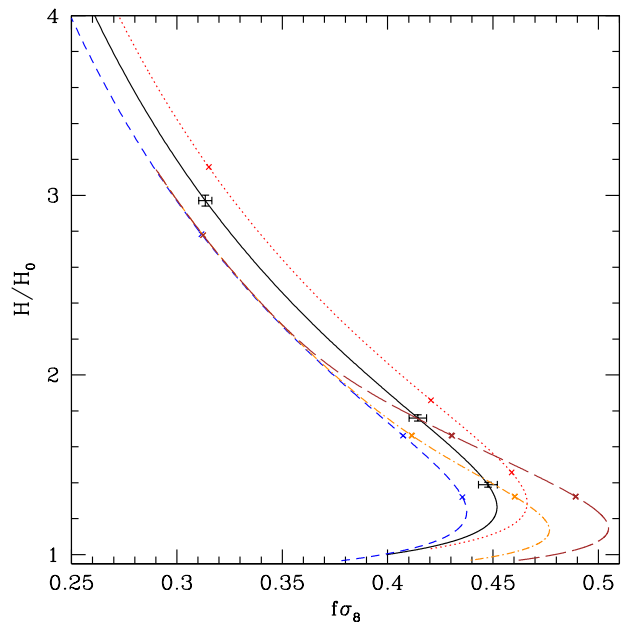


FIG. 5. As Fig. 4 but showing a modified gravity model instead of the dark energy w curves. The modified gravity curves are for an exponential $f(R)$ gravity model and exhibit scale dependence in growth, with a clear difference between wave numbers $k = 0.02 h/\text{Mpc}$ (orange, dot-dash curve) and $k = 0.1 h/\text{Mpc}$ (brown, long dashed curve). The $f(R)$ model has an expansion history equivalent to $\Omega_m = 0.28$ Λ CDM (blue, short dashed curve), but a very different growth history.

quickly the extra density (the superdeceleration), and a restoration to $w = -1$ at more recent times. The enhanced dark energy density reduces the source term in the growth equation and suppresses growth. This causes a “stutter” in growth, where basically the momentum of the growth (δ) drops significantly as matter domination wanes and the enhanced dark energy density comes into play. Even though the conditions after the step back down to $w = -1$ are identical to low redshift Λ CDM, the growth has been stunted and takes time to recover.

The results in Fig. 6 show the impact of this model. We choose a step of length $N = 0.2 e$ -folds ending at $z_d = 2$, falling in the middle of the allowed region of Fig. 5 in [23]. Too long a period of superdeceleration, at too recent an epoch, changes the CMB distance to last scattering and causes an excessive integrated Sachs-Wolfe effect (see [20, 23] for detailed discussion of the physical effects). Growth is indeed suppressed for nearly the same expansion history over the range of redshifts plotted. The wiggle now is pushed to the left, from the rightmost standard curve (we use this model with $\Omega_m = 0.32$) toward those with lower matter density.

To understand the behavior, note that at high redshift, well above the transition in behavior, there is enhanced dark energy density (by a factor e^{6N}). During the matter dominated regime, this has little effect and the su-

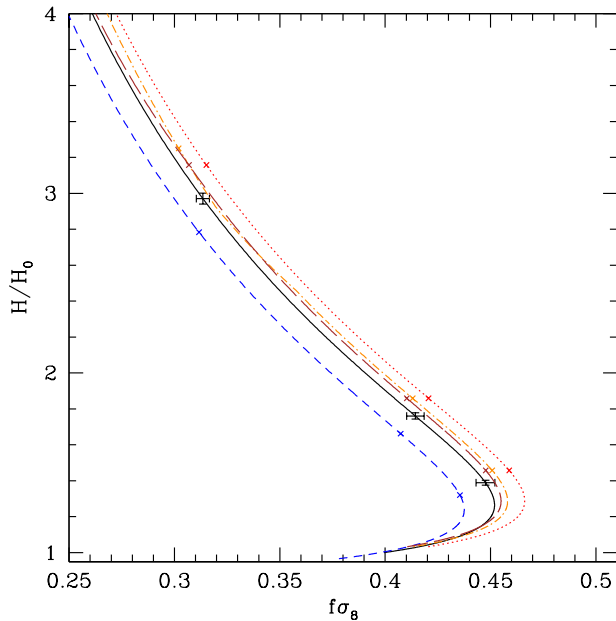


FIG. 6. As Fig. 4 but showing a suppressed growth superdecelerating model instead of the dark energy w curves. The stunted growth curves show results from $N = 0.2$ e -folds of superdeceleration at $z_d = 2$ (brown, long dashed curve) and $N = 0.1$ at $z_d = 1.5$ (orange, dot-dash curve), both in accord with CMB distance to last scattering measurements and having $\Omega_m = 0.32$. At redshifts below the transition redshift, the expansion history is identical to that of $\Omega_m = 0.32$ LCDM and the expansion vs growth curves gradually become horizontal offsets of that model, as the growth rate recovers at a suppressed growth amplitude.

perdecelerating models used join the standard $\Omega_m = 0.32$ curve. However, the enhanced dark energy density (and hence lower matter density for a flat universe) has more of an impact on expansion and growth at higher redshift than the standard model, increasing the expansion rate but slowing the growth rate, and the conjoint history curve begins to bend to the left, acting as reduced matter density curves in both expansion and growth. Indeed, if a period of early dark energy domination were allowed to occur, then the growth rate would approach zero. However, such a strong effect would leave clear signatures in the CMB (see [20, 23]) and is ruled out by current measurements.

During the e -folds of superdeceleration, the dark energy density drops; to preserve the same value of dark energy density today, a larger number N of e -folds implies higher early dark energy density, so N is tightly constrained. After the superdeceleration period ends, the expansion history is identical to that of the corresponding matter density model, and the growth rate can recover from its “stutter” where the momentum of growth $\dot{\delta}$ was suppressed, but the amplitude of growth σ_8 is at a lower level. Overall this shifts the conjoint history tracks of these models to the left, roughly parallel to the standard

cosmology track. This can lead to degeneracy with lower matter density standard cosmologies (e.g. $\Omega_m \approx 0.31$ for the case shown in Fig. 6) – unless the histories are measured out to sufficiently high redshift near the transition, or accurately at low redshift $z \lesssim 0.5$ below the wiggle where different standard cosmology tracks are not parallel.

Thus, the conjoint histories diagram appears to be an effective method for understanding the behavior of expansion and growth viewed together, and distinguishing models both within standard cosmology, and especially those that deviate from it by enhancing or suppressing growth, e.g. through modified gravity or a stutter in sourcing growth. Moreover, it highlights the different and mutually supportive roles of expansion and growth measurements near the wiggle ($z \approx 0.5$), at low redshift $z \lesssim 0.5$, and at high redshift $z \approx 2-3$ to identify the cosmological physics.

IV. FUTURE CONSTRAINTS

Future spectroscopic surveys will use galaxy and quasar clustering to measure the expansion rate H and growth rate $f\sigma_8$ with subpercent precision over a wide range of redshift. For example, DESI will extend up to $z \approx 1.5$ with galaxies and can reach higher redshift with quasars and the Lyman- α forest, while Euclid and WFIRST will cover $z \approx 1-2.5$ at such precision [24, 25]. We have indicated in Figs. 4, 5, and 6 the 1σ constraints assuming 1% measurements of each quantity at various redshifts (treating them approximately as uncorrelated since H arises from radial BAO and $f\sigma_8$ from redshift space distortions, using different scales in the data; the qualitative conclusions do not depend strongly on this).

Obtaining highly accurate growth measurements at $z \gtrsim 3$ will be challenging, but useful for breaking degeneracies between models. An intriguing area for further concentration is the low redshift regime, $z \lesssim 0.5$, where the wiggle peaks and then the conjoint history curves change shape. Surveys are beginning to map substantial fractions of the available volume here, and peculiar velocity surveys such as the TAIPAN survey or perhaps future supernova surveys may map the growth rate [26–28], although the restricted volume limits the attainable precision.

V. CONCLUSIONS

The cosmic expansion and cosmic growth histories are fundamental observables describing our universe. Current surveys are taking the first steps at mapping these over substantial parts of the recent history, and future surveys will greatly expand this in range and accuracy. While these two quantities, $H(z)$ and $f\sigma_8(z)$, as a function of redshift contain the cosmological information, viewing them simultaneously as a conjoint constraint

can illuminate important aspects of the overall cosmic evolution, especially for cases that go beyond standard models within general relativity.

The conjoined approach can aid in interpretation, e.g. clearly recognizing enhanced or suppressed growth for a given expansion history, or identifying particular redshift ranges of interest. The swing, or wiggle, in the conjoined diagram highlights a time of greater sensitivity to the cosmological model, and the regions of high and low redshift can also identify and point to methods of breaking covariances between parameters.

We exhibited the joint history tracks for four models: a standard constant dark energy equation of state, a time varying dark energy equation of state that matches the CMB distance to last scattering, a modified gravity model than enhances growth – in a scale dependent manner, and a stuttering, superdecelerating model that suppresses growth. We discussed the physical effects and sensitive redshift range of each, with some altering both expansions and growth histories, some changing only one. In particular, the modified gravity model tracks showed a wiggle extending outside the standard model band. An alternate approach of convolving the expansion and growth observables into a single function $f\sigma_8 H^{2/3}$ had the interesting property that it must go to a well deter-

mined constant at high redshift for any cosmology with a matter dominated epoch.

The redshift ranges of particular interest are those near the wiggle, i.e. the range $z \approx 0.5-1$ at which surveys will excel, but also $z \lesssim 0.5$ for which upcoming peculiar velocity surveys such as TAIPAN and those using highly calibrated supernovae will offer a new window. Finally, the epochs at $z \gtrsim 3$, perhaps accessible in the future through 21 cm surveys, could play a useful role in breaking degeneracies and carrying out a robust consistency test of early matter domination. Contrasting and conjoining cosmic expansion and growth histories provides a fundamental test of general relativity and insight into the intertwined evolution of spacetime as a whole and the large scale structure within it.

ACKNOWLEDGMENTS

I thank the Aspen Center for Physics, which is supported by NSF grant PHY-1066293, for a motivating environment. This work is supported in part by the Energetic Cosmos Laboratory and by the U.S. Department of Energy, Office of Science, Office of High Energy Physics, under Award DE-SC-0007867 and contract no. DE-AC02-05CH11231.

-
- [1] S. Alam et al., [arXiv:1607.03155](#)
 - [2] M. Vargas-Magaña et al., [arXiv:1610.03506](#)
 - [3] Z. Li, Y.P. Jing, P. Zhang, D. Cheng, [arXiv:1609.03697](#)
 - [4] G.B. Zhao et al., [arXiv:1607.03153](#)
 - [5] F. Beutler et al., [arXiv:1607.03150](#)
 - [6] F. Beutler et al., [arXiv:1607.03149](#)
 - [7] S. Satpathy et al., [arXiv:1607.03148](#)
 - [8] A.G. Sanchez et al., [arXiv:1607.03147](#)
 - [9] A.J. Ross et al., [arXiv:1607.03145](#)
 - [10] J.N. Grieb et al., [arXiv:1607.03143](#)
 - [11] H. Gil-Marín et al., [arXiv:1606.00439](#)
 - [12] C. Contreras et al., *Mon. Not. Roy. Astron. Soc.* 430, 924 (2013) [[arXiv:1302.5178](#)]
 - [13] D. Parkinson et al., *Phys. Rev. D* 86, 103518 (2013) [[arXiv:1210.2130](#)]
 - [14] C. Blake et al., *Mon. Not. Roy. Astron. Soc.* 425, 405 (2012) [[arXiv:1204.3674](#)]
 - [15] E.V. Linder, M. Oh, T. Okumura, C.G. Sabiu, Y-S. Song, *Phys. Rev. D* 89, 063525 (2014) [[arXiv:1311.5226](#)]
 - [16] Y-S. Song, C.G. Sabiu, T. Okumura, M. Oh, E.V. Linder, *J. Cos. Astropart. Phys.* 1412, 005 (2014) [[arXiv:1407.2257](#)]
 - [17] Y-S. Song et al., *Phys. Rev. D* 92, 043522 (2015) [[arXiv:1507.01592](#)]
 - [18] F. Beutler et al., *Mon. Not. Roy. Astron. Soc.* 443, 1065 (2014) [[arXiv:1312.4611](#)]
 - [19] L. Samushia et al., *Mon. Not. Roy. Astron. Soc.* 439, 3504 (2014) [[arXiv:1312.4899](#)]
 - [20] E.V. Linder and T.L. Smith, *J. Cos. Astropart. Phys.* 1104, 001 (2011) [[arXiv:1009.3500](#)]
 - [21] E.V. Linder, [arXiv:0708.0224](#)
 - [22] E.V. Linder, *Phys. Rev. D* 80, 123528 (2009) [[arXiv:0905.2962](#)]
 - [23] E.V. Linder, *Phys. Rev. D* 82, 063514 (2010) [[arXiv:1006.4632](#)]
 - [24] A. Font-Ribera, P. McDonald, N. Mostek, B.A. Reid, H-J. Seo, A. Slosar, *J. Cos. Astropart. Phys.* 1405, 023 (2014) [[arXiv:1308.4164](#)]
 - [25] D. Weinberg, D. Bard, K. Dawson, O. Doré, J. Frieman, K. Gebhardt, M. Levi, J. Rhodes, [arXiv:1309.5380](#)
 - [26] C. Howlett, L. Staveley-Smith, C. Blake, [arXiv:1609.08247](#)
 - [27] I. Odderskov and S. Hannestad, [arXiv:1608.04446](#)
 - [28] A. Johnson et al., *Mon. Not. Roy. Astron. Soc.* 444, 3926 (2014) [[arXiv:1404.3799](#)]